CAD Models for Multilayered Substrate Interdigital Capacitors

Spartak S. Gevorgian, *Member, IEEE*, Torsten Martinsson, Peter L. J. Linnér, *Senior Member, IEEE*, and Erik Ludvig Kollberg, *Fellow, IEEE*

***Abstract*—Conformal mapping-based models are given for interdigital capacitors on substrates with a thin superstrate and/or covering dielectric film. The models are useful for a wide range of dielectric constants and layer thicknesses. Capacitors with finger numbers $n \geq 2$ are discussed. The finger widths and spacing between them may be different. The results are compared with the available data and some examples are given to demonstrate the potential of the models.**

I. Introduction

INTERDIGITAL capacitors (IDC) are widely used as lumped elements in microwave integrated circuits (MIC) [1], [2], slow-wave devices [3], integrated optical (IO) modulators, deflectors [4], and thin-film acoustoelectronic transducers [5]. Recently, the integration of high temperature superconductor (HTSC) and ferroelectric films [6], [7] has initiated a renewed interest toward the electrically tunable devices based on interdigital capacitors [8]. Full wave analysis of interdigital capacitors on homogeneous or multilayer substrates is a complex computational problem, while for syntheses of MIC or IO devices there is a need for closed form analytical expressions for computation of the capacitances of IDC. The available analytical solutions [1], [9] are limited to homogeneous substrates and equal finger and slot widths. Recently, simple formulas have been proposed for IDC with a dielectric layer on top of thin conducting strips [8]. These formulas do not take into account the fringing field of the finger ends, and lead to higher capacitances in comparison with the widely used formulas [1], [9].

In this paper, the conformal mapping technique is used to evaluate closed form expressions for computation of capacitances of IDC on two- and three-layered substrates. The derivation is based on the partial capacitance method [2], [10]–[12] and takes into account the capacitance between the fingers and the fringing capacitance of the finger ends.

IDC with $n \geq 2$ fingers are discussed. Capacitances of all capacitors are presented as a sum of capacitances between the fingers and capacitances of the finger ends. The main part, the capacitances between the regular sections of the fingers, are evaluated accurately in Sections III–V. A special conformal mapping technique is developed for IDC with $n \geq 4$. Capacitances of two- and three-strip IDC are easily evaluated using available formulas for the capacitances of a coplanar strip [12], [13] and coplanar waveguide [11], [12] on substrates of limited thickness and the partial capacitance technique presented in [10]. For IDC with fingers much longer than the width, the "end" capacitance is a small fraction of the total capacitance. In Section VI, simple analytical approximations are proposed for this "end" capacitance which can be used for all IDC with $n \geq 2$ discussed in this paper.

It is assumed that the microwave wavelength in the substrate is much larger than the dimensions of the IDC. The models do not take into account parasitic inductances and resistances.

Manuscript received September 14, 1995; revised February 15, 1996 This work was supported by the Swedish National Board of Industrial and Technical Development

The authors are with the Department of Microwave Technology, Chalmers University of Technology, Gothenburg, Sweden.

Publisher Item Identifier S 0018-9480(96)03801-X.

II. Physical Models of IDC

IDC layouts and cross sections to be discussed are shown in Fig. 1. All slots are assumed to have a width of $2g$ and the finger width is $2s$. External strips may have widths, $2s_1$, different from the widths of the internal strips, $2s$. Wheeler's first order approximation [2] is applied to account for the thickness, t, of the strips. The effective width of the strips are presented as follows:

$$2s = 2s_g + \left(\frac{t}{\pi}\right)\left[1 + \ln\left(\frac{8\pi s_g}{t}\right)\right] \tag{1}$$

where $2s_g$ is the physical (geometric) width of the strip. Designs with infinite width terminals, Fig. 1(a), and finite width terminals, w, Fig. 1(b), will be discussed. In general, the width of the slots between fingers, $2g$, is not equal to the width of the strips, $2s$. The gaps at the ends of the fingers, $2g_{\text{end}}$, may also be different.

The dielectric constants of the substrate, ϵ_1, superstrate, ϵ_2, and cover layer, ϵ_3, may have arbitrary values including $\epsilon_1 > \epsilon_2$. The thickness of the substrate is larger than the thickness of the superstrate, $h_1 > h_2$. In Fig. 2, the finger potential and the schematics of the field lines for IDC with $n \geq 3$, two, and three fingers are presented. Although the symmetric field distribution shown in Fig. 2(a) is valid only for an infinite number of fingers, we will assume a similar distribution for a finite number of fingers, including $n \geq 4$. All dielectric/dielectric and dielectric/air interfaces are modeled as equivalent magnetic walls as it is usually done in the partial capacitance technique [2], [10]–[12]. Additionally, electric walls are assumed at the symmetry planes of the electric field distribution, where the field lines are normal to the electric wall.

It follows from the electric field distribution and the symmetry of the capacitance structures, Fig. 2, that the capacitances

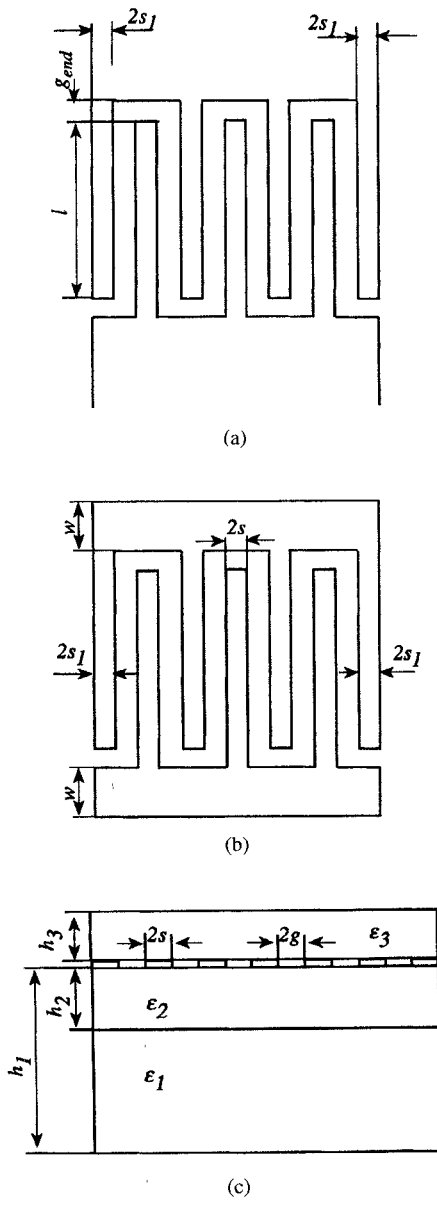

Fig. 1. Layouts (a), (b), and cross section (c) of the interdigital capacitors.

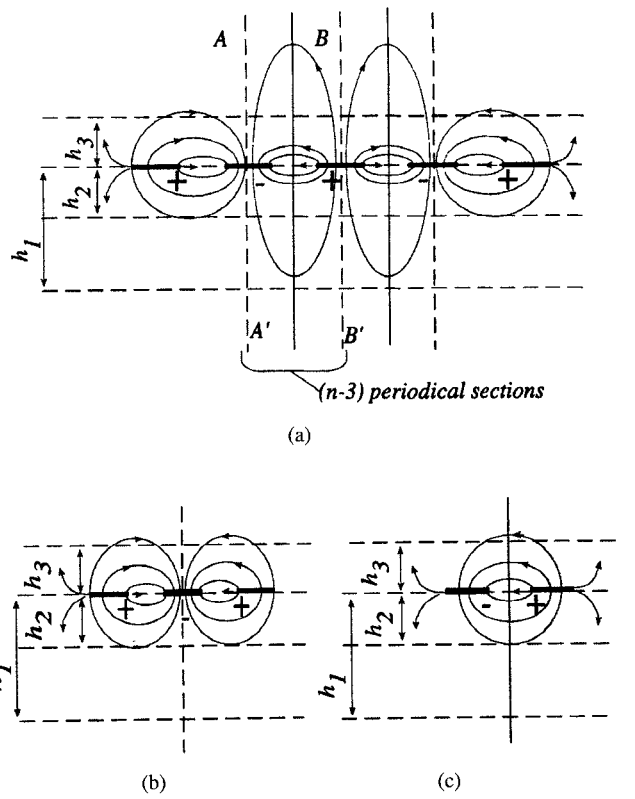

Fig. 2. Potential distribution and schematics of electric field distribution in periodical (a), three-finger IDC (b), and two-finger IDC (c).

of two- and three-finger capacitors, C_2 and C_3, have to be analyzed separately. The capacitance of an IDC with $n \geq 3$ may be presented as the sum of a capacitance of a three-finger capacitor, C_3, and the capacitances of periodical $(n-3)$ structures, C_n, enclosed between the magnetic walls AA' and BB', Fig. 2(a), and a correction term for the fringing fields of the ends of the strips, C_{end}

$$C = C_3 + C_n + C_{\text{end}}. \tag{2}$$

III. The Capacitance of the Periodical Section

A. Single-Layer Substrate

Before evaluation of the capacitance of one section of the periodical structure on a three-layered substrate, Fig. 2(a), consider the simple case of a single-layer substrate with thickness h and dielectric constant ϵ, Fig. 3. It follows from the schematic field distribution, Fig. 3(a), that the partial capacitance between half strips, s, of neighboring fingers due to the substrate is equal to the capacitance between one of the half strips and virtual equipotential strip of height h laying in the electric wall CC', line section $\overline{25}$. This configuration is conveniently represented in Fig. 3(b). Now the problem is to evaluate the capacitance between the line segments (strips) s and h of the polygon $\overline{0256}$ in the Z-plane, Fig. 3(b). The standard procedure [15] for evaluation of this capacitance suggests an application of the Schwartz–Chrisoffel transformation to map the polygon $\overline{0256}$ onto a half plane of an intermediate plane. Then the second application of Schwartz–Christoffel transformation maps this intermediate half plane onto the interior of the desired rectangle to form a parallel-plate capacitor for calculation of the capacitance. This procedure leads to complex expressions involving both Jacobian elliptic functions (from the first transformation) and elliptic integrals (from the second transformation) [15]–[17]. On the other hand, it follows from the study of the field distribution and the equivalent magnetic and electric walls, Fig. 3(a) and (b), that the field line configuration will not be changed if one assumes a semi-infinite perfect metal strip behind the segment of the line $\overline{25}$ in the z-plane, Fig. 3(b). Thus, instead of a Schwartz–Chrisoffel integral-assisted mapping of the interior of the rectangle $\overline{0256}$, we map the semi-infinite strip (triangle) $\overline{3064}$ of the Z-plane on the upper half of the T-plane, Fig. 3(c), using the function

$$T = \cosh^2\left(\frac{\pi z}{2h}\right). \tag{3}$$

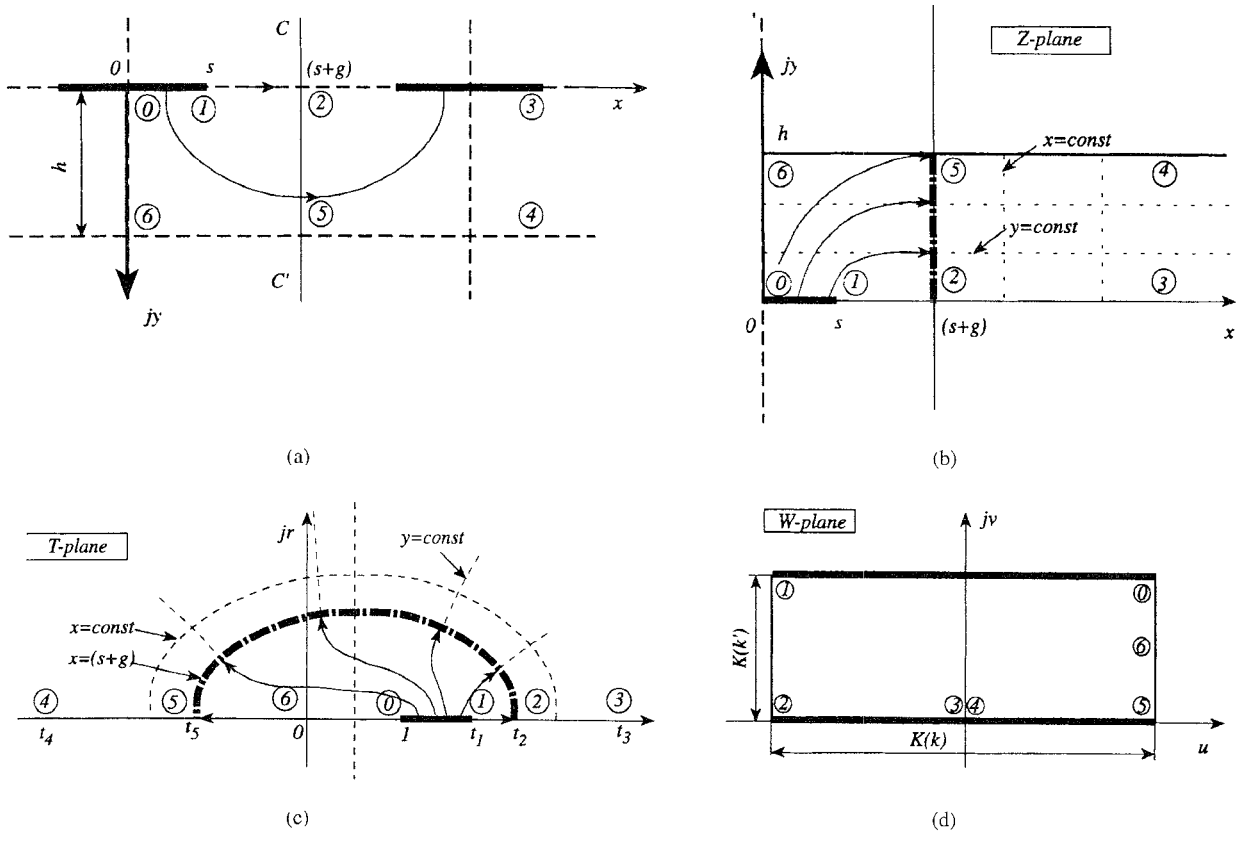

Fig. 3. A section of a periodical structure (a), and its mapped planes (b), (c), (d).

The schematics of the field line configuration which resulted from this transformation are shown in Fig. 3(c). The vortices of the mapped polygon in the T-plane are

$$t_0 = 1, \quad t_1 = \cosh^2\left(\frac{\pi s}{2h}\right), \quad t_3 = t_4 = \infty,$$
$$t_5 = -\sinh^2\left(\frac{\pi(s+g)}{2h}\right), \quad t_6 = 0.$$

Next, for the thin-film limit, exploiting the technique of approximate transformations ([15, ch. 4]), we map the upper half of the T-plane onto the interior of the rectangle in W-plane, Fig. 3(d). The mapping function is

$$w = A\int_t^{t_5} \frac{dt}{\sqrt{(1-1)(t-t_1)(t-t_2)(t-t_5)}} + B. \quad (4)$$

Constants A and B are determined from the correspondence of the vortices in the T- and W-planes. This procedure leads to the following expression for the capacitance per unit length:

$$C_{n1} = \frac{1}{2}\epsilon\epsilon_0\frac{K(k)}{K(k')}. \quad (5)$$

The coefficient 1/2 is due to the identical capacitance between the virtual strip $\overline{25}$, Fig. 3(a), and the next half strip, s. These capacitances are in series. The modulus of the elliptic integrals of the first kind $K(k)$ and $K(k')$, are evaluated using the t_i values given above based on the presentation given in [18]

$$k = \frac{\sinh\left(\frac{\pi s}{2h}\right)}{\sinh\left(\frac{\pi(s+g)}{2h}\right)} \cdot \sqrt{\frac{\cosh^2\left(\frac{\pi(s+g)}{2h}\right) + \sinh^2\left(\frac{\pi(s+g)}{2h}\right)}{\cosh^2\left(\frac{\pi s}{2h}\right) + \sinh^2\left(\frac{\pi(s+g)}{2h}\right)}} \quad (6)$$

$k' = \sqrt{1-k^2}$.

The capacitance per unit length between the neighboring strips limited by magnetic walls, Fig. 3(a), in the absence of the substrate, is found from (5) and (6) as limiting case, where $\epsilon = 1, h = \infty$

$$C_{n0} = \epsilon_0\frac{K(k_0)}{K(k_0')} \quad (7)$$

$$k_0 = \frac{s}{s+g}. \quad (8)$$

In (7), the capacitances due to the upper and lower half air spaces in the Z-plane are taken into account.

B. Three-Layered Substrate

Now we use the results of the previous subsection to evaluate the capacitance of the $(n-3)$ periodical sections of the IDC on a three-layered substrate. Following the partial capacitance technique [10], this capacitance may be presented

as a sum of partial capacitances due to the i) air filling (7), ii) substrate, C_{n1}, and iii) superstrate, C_{n2}, and the cover layer, C_{n3}

$$C_n = (n-3)(C_{n0} + C_{n1} + Cn_{n2} + C_{n3})l. \tag{9}$$

C_{n1}, C_{n2}, and C_{n3} are determined by (5), where h_1, h_2, and h_3 are the substrate thicknesses used, with the equivalent dielectric constants $(\epsilon_1 - 1), (\epsilon_2 - \epsilon_1)$ and $(\epsilon_3 - 1)$. The resultant capacitance is

$$C_n = (n-3)\epsilon_3\epsilon_{en}\frac{K(k_0)}{K(k_0')}l \tag{10}$$

where

$$\epsilon_{en} = 1 + q_{1n}\frac{\epsilon_1 - 1}{2} + q_{2n}\frac{\epsilon_2 - \epsilon_1}{2} + q_{3n}\frac{\epsilon_3 - 1}{2} \tag{11}$$

$$q_{in} = \frac{K(k_{in})}{K(k_{in}')}\frac{K(k_0')}{K(k_0)} \tag{12}$$

$$k_{in} = \frac{\sinh\left(\frac{\pi s}{2h_i}\right)}{\sinh\left(\frac{\pi(s+g)}{2h_i}\right)} \cdot \sqrt{\frac{\cosh^2\left(\frac{\pi(s+g)}{2h_i}\right) + \sinh^2\left(\frac{\pi(s+g)}{2h_i}\right)}{\cosh^2\left(\frac{\pi s}{2h_i}\right) + \sinh^2\left(\frac{\pi(s+g)}{2h_i}\right)}}. \tag{13}$$

$i = 1, 2, 3$, and l is the finger length.

In the $s/h_i \gg 1$ limit, the last expression is simplified to

$$k_i = \sqrt{2}\exp\left(-\frac{\pi g}{2h_i}\right) \tag{14}$$

$k_i' = \sqrt{1 - k_i^2}$. It is supposed that the condition $h_1 \geq h_2$ is fulfilled where the dielectric layer 2 is enclosed between strips and substrate.

The contribution from the other three external fingers [one and a half on each side, Fig. 2(a)] will be taken into account as a capacitance of three-strip coplanar waveguide discussed in the next Section.

IV. The Capacitance of the Three Finger Section

A. Finite Width Strips

To evaluate the capacitance of a three-finger IDC, Fig. 4, on a two-layered substrate, we use available formulas for three strips on a single-layer substrate [12]. Similar results can be found in [11]. In general, the widths of the external strips, $2s_1$, are not the same as the width of central the strips, $2s$. As in the previous cases, the capacitance of a three-finger IDC is assumed to be a sum of partial capacitances due to air, substrate with an equivalent dielectric constant $(\epsilon_1 - 1)$, and superstrate with a dielectric constant $(\epsilon_2 - \epsilon_1)$, and cover layer with equivalent dielectric constant $(\epsilon_3 - 1)$. The resultant capacitance is

$$C_3 = 4\epsilon_0\epsilon_{e3}\frac{K(k_{03}')}{K(k_{03})}l \tag{15}$$

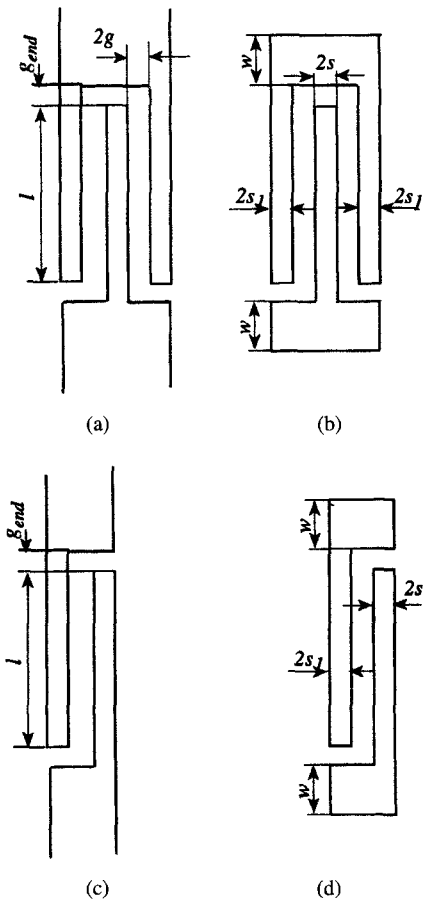

Fig. 4. Layouts of three-finger IDC (a), (b), and two-finger IDC (c), (d) .

where

$$\epsilon_{e3} = 1 + q_{13}\frac{\epsilon_1 - 1}{2} + q_{23}\frac{\epsilon_2 - \epsilon_1}{2} + q_{33}\frac{\epsilon_3 - 1}{2} \tag{16}$$

$$q_{i3} = \frac{K(k_{i3})}{K(k_{i3}')}\frac{K(k_{03}')}{K(k_{03})}, \qquad i = 1, 2 \tag{17}$$

$$k_{03} = \frac{s}{s+2g}\sqrt{\frac{1 - \left(\frac{(s+2g)}{(s+2s_1+2g)}\right)^2}{1 - \left(\frac{s}{(s+2s_1+2g)}\right)^2}} \tag{18}$$

$$k_{i3} = \frac{\sinh\left(\frac{\pi s}{2h_i}\right)}{\sinh\left(\frac{\pi(s+2g)}{2h_i}\right)} \cdot \sqrt{\frac{1 - \sinh^2\left[\frac{\pi(s+2g)}{2h_i}\right] \Big/ \sinh^2\left[\frac{\pi(s+2s_1+2g)}{2h_i}\right]}{1 - \sinh^2\left[\frac{\pi s}{2h_i}\right] \Big/ \sinh^2\left[\frac{\pi(s+2s_1+2g)}{2h_i}\right]}} \tag{19}$$

$k_{i3}' = \sqrt{1 - k_{i3}^2}, i = 1, 2, 3$. In the above formula, $s_1 = s$ should be used where the widths of external and middle fingers are the same.

B. Infinite Width External Strips

Let us assume that the external strips, Fig. 1(a) and (b), are extended to infinity. In this case, the capacitance is easily deduced from (15)–(19) by performing limiting transformations where $2s_1 \to \infty$

$$C_{3\infty} = 4\epsilon_0\epsilon_{e3\infty}\frac{K(k'_{30\infty})}{K(k_{30\infty})}l \tag{20}$$

where

$$\epsilon_{e3\infty} = 1 + q_{13\infty}\frac{\epsilon_1 - 1}{2} + q_{23\infty}\frac{\epsilon_2 - \epsilon_1}{2} + q_{33\infty}\frac{\epsilon_3 - 1}{2} \tag{21}$$

$$q_{i3\infty} = \frac{K(k_{i3\infty})}{K(k'_{ie\infty})}\frac{K(k'_{03\infty})}{K(k_{03\infty})}. \tag{22}$$

$$k_{03\infty} = \frac{s}{s+2g} \tag{23}$$

$$k_{i3\infty} = \frac{\sinh\left(\frac{\pi s}{2h_i}\right)}{\sinh\left(\frac{\pi(s+2g)}{2h_i}\right)} \qquad i = 1,2,3 \tag{24}$$

V. The Capacitance of a Two-Finger Section

A. Asymmetric Strips

For an asymmetric two-finger capacitor, Fig. 4(b), with stripwidths $2s, 2s_1$, and gapwidth $2g$ using the results [13] we arrive for three-layered substrate to

$$C_{2a} = 2\epsilon_0\epsilon_{e2a}\frac{K(k_{02a})}{K(k'_{02a})}l \tag{25}$$

$$\epsilon_{e2a} = 1 + q_{12a}\frac{\epsilon_1 - 1}{2} + q_{22a}\frac{\epsilon_2 - \epsilon_1}{2} + q_{32a}\frac{\epsilon_3 - 1}{2} \tag{26}$$

$$q_{i2a} = \frac{K(k_{i2a})}{K(k'_{i2a})}\frac{K(k'_{02a})}{K(k_{02a})}, \qquad i = 1,2,3 \tag{27}$$

$$k_{02a} = \sqrt{\frac{s}{s+g}\frac{s_1}{s_1+g}} \tag{28}$$

$$k_{i2a} = \sqrt{\frac{\sinh\left(\frac{\pi s}{2h_i}\right)}{\sinh\left(\frac{\pi(s+g)}{2h_i}\right)}\frac{\sinh\left(\frac{\pi s_1}{2h_i}\right)}{\sinh\left(\frac{\pi(s_1+g)}{2h_i}\right)}}, \qquad i = 1,2,3. \tag{29}$$

B. Symmetric Strips

Conformal mapping-based formulas for the capacitance of two strips of the same width on a finite thickness substrate are given in [14]. Application of these formulas to three-layer substrate two-finger IDC leads to

$$C_{2s} = 2l\epsilon_0\epsilon_{e2s}\frac{K(k'_{20s})}{K(k_{20s})} \tag{30}$$

$$\epsilon_{e2s} = 1 + q_{12s}\frac{\epsilon_1 - 1}{2} + q_{22s}\frac{\epsilon_2 - \epsilon_1}{2} + q_{32s}\frac{\epsilon_3 - 1}{2} \tag{31}$$

$$q_{i2s} = \frac{K(k'_{i2s})}{K(k_{i2s})}\frac{K(k_{02s})}{K(k'_{02s})}, \qquad i = 1,2,3 \tag{32}$$

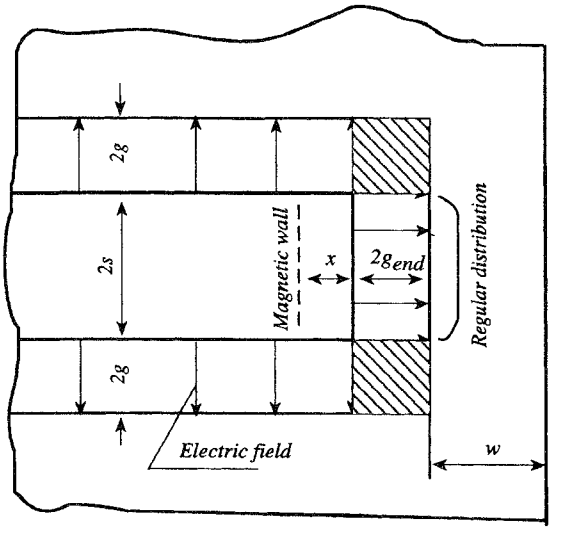

Fig. 5. A model of a finger end

$$k_{02s} = \frac{g}{g+2s} \tag{33}$$

$$k_{i2} = \frac{\sinh\left(\frac{\pi g}{2h_i}\right)}{\sinh\left(\frac{\pi(2s+g)}{2h_i}\right)}, \qquad i = 1,2,3. \tag{34}$$

VI. The Capacitance Due to the Finger Ends

For long fingers, $l/s \gg 1$, the results presented above can be used for IDC capacitance computations without taking into account the correction for the fringing fields at the ends of the fingers, as it has been done in [5] and [8]. Then, the accuracy of the computed capacitance is limited to 5–10%. Nevertheless, some simple formulas will be given below for the "end" capacitances associated with the fringing fields between the ends of the fingers and the leads.

A. Finite Width Teminals

First we start with finite width, w, terminals, Fig. 1(b). A fragment of the end of a finger is shown in Fig. 5. The actual field distribution is complex. It is still possible to use the conformal mapping technique to compute this field distribution and the associated finger end capacitance [22]. Nevertheless, these results are complex and do not improve substantially the accuracy of the total capacitance of the IDC in comparison with the simpler models presented below. As a first approximation, we assume a region with a regular field distribution neighboring the end of the finger strip and two nonregular regions (dashed in Fig. 5) near the corners. Thus, we can put a virtual magnetic wall at the distance x from the end of the finger, Fig. 5, and compute the "regular end" capacitance as half of the capacitance of the three-strip structure, Section IV-A, assuming external strips of width $2s_1 = w$ and a central strip of width $2s = 2x$, separated by a gap $2g_{\text{end}}$. As a first approach, the two corners near the end of each finger are approximated as a πs extension to the

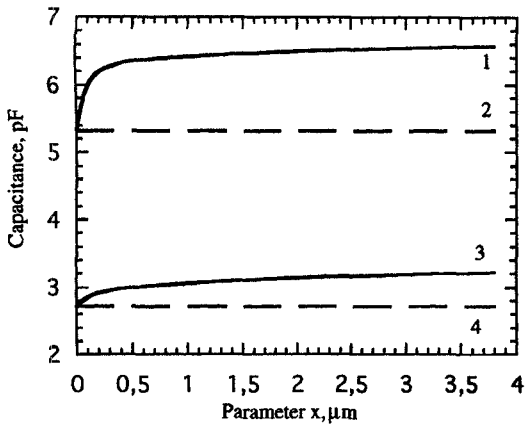

Fig. 6. Dependence of the total capacitance of the IDC on parameter x.

finger width. The end capacitance of the n fingers is

$$C_{\text{end}} = 4ns(2+\pi)\epsilon_0\epsilon_{e\text{end}}\frac{K(k_{0\text{end}})}{K(k'_{0\text{end}})} \tag{35}$$

where

$$\epsilon_{\text{end}} = 1 + q_{1\text{end}}\frac{\epsilon_1 - 1}{2} + q_{2\text{end}}\frac{\epsilon_2 - \epsilon_1}{2} + q_{3\text{end}}\frac{\epsilon_3 - 1}{2} \tag{36}$$

$$k_{0\text{end}} = \frac{x}{x+2g_{\text{end}}}\sqrt{\frac{1-\left(\dfrac{(x+2g_{\text{end}})}{(x+w+2g_{\text{end}})}\right)^2}{1-\left(\dfrac{x}{(x+w+2g_{\text{end}})}\right)^2}}. \tag{38}$$

B. Infinite Width Terminals

For infinite width terminals, Fig. 1(a), the finger-end capacitance is obtained from the results of the previous subsection in the $w \to \infty$ limit

$$C_{\text{end}\infty} = 4ns(2+\pi)\epsilon_0\epsilon_{\text{end}\infty}\frac{K(k_{0\text{end}\infty})}{K(k'_{0\text{end}\infty})} \tag{39}$$

$$\epsilon_{\text{end}\infty} = 1 + q_{1\text{end}\infty}\frac{\epsilon_1 - 1}{2} + q_{2\text{end}\infty}\frac{\epsilon_2 - \epsilon_1}{2} + q_{3\text{end}\infty}\frac{\epsilon_3 - 1}{2} \tag{40}$$

$$q_{i\text{end}\infty} = \frac{K(k_{i\text{end}\infty})}{K(k'_{i\text{end}\infty})}\frac{K(k'_{0\text{end}\infty})}{K(k_{0\text{end}\infty})}, \qquad i = 1,2,3 \tag{41}$$

$$k_{0\text{end}\infty} = \frac{x}{x+2g_{\text{end}}} \tag{42}$$

$$k_{i\text{end}} = \frac{\sinh\left(\dfrac{\pi x}{2h_i}\right)}{\sinh\left(\dfrac{\pi(x+g_{\text{end}})}{2h_i}\right)}, \qquad i = 1,2,3. \tag{43}$$

For most practical cases, the finger length is much greater than the finger width and the end capacitance is a small fraction of the total capacitance of IDC. One can expect from the field distribution at the end of the fingers [22] that $x \leq s$ for $s \equiv g$. An example of the dependence of the total capacitance on x is depicted in Fig. 6. The data used in Fig. 6 is as follows: $\epsilon_2 = \epsilon_1 = 24.5, n = 60, l = 0.5$ mm, $2s = 2g = 7.6$ μm, $t = h2 = 0.3$ μm, $\epsilon_3 = 265$ (curves 1 and 2), $\epsilon_3 = 1$ (curves 3 and 4). The sharp increase in capacitance for small x is followed by a saturation near $x = 0.5s$. The electric field component normal to the surface of the strips decreases substantially at this distance. This value of x leads to the best agreement when the computed capacitances are compared with the results of other models and experiment. For comparison, we treat the end of a finger, Fig. 5, as an open end of a coplanar waveguide. The total end capacitance of 60 fingers computed using Mao's model [21] for $\epsilon_3 = 1$ is 0.435 pF, while from formula (39) we have 0.414 pF assuming $x = 0.5s$.

For shorter finger lengths, $1 \leq 2s$, the contribution of the "end" capacitance to the total capacitance is larger and it has to be treated more accurately. More accurate values of x may be determined from the full wave analysis or experiment.

VII. Limiting Cases and Discussions

In this Section, we give a brief summary of the formula for capacitances of a variety of IDC. Comparisons with experimental and theoretical results available in the literature are given. Some numerical data are presented to demonstrate the potential of the models developed in this paper.

A. Summary of Formulas for IDC Capacitances

IDC with finger number $n \geq 4$:

1) IDC with finite width external fingers and finite width terminals, Fig. 1(b):
$$C = C_n + C_3 + C_{\text{end}}. \tag{44}$$
2) IDC with infinite width external fingers and finite width terminals:
$$C = C_n + C_{3\infty} + C_{\text{end}}. \tag{45}$$
3) IDC with finite width external fingers and infinite width terminals, Fig. 1(a):
$$C = C_n + C_3 + C_{\text{end}\infty}. \tag{46}$$
4) IDC with infinite width external fingers and infinite width terminals:
$$C = C_n + C_{3\infty} + C_{\text{end}\infty}. \tag{47}$$

IDC with finger number $n = 3$:

1) Finite width external fingers and finite width terminals, Fig. 4(b):
$$C = C_3 + C_{\text{end}}. \tag{48}$$
2) Infinite width external fingers and finite width terminals:
$$C = 3_{3\infty} + C_{\text{end}}. \tag{49}$$
3) Finite width external fingers and infinite width terminals, Fig. 4(a):
$$C = C_3 + C_{\text{end}\infty} \tag{50}$$
4) Infinite width external fingers and infinite width terminals:
$$C = C_{3\infty} + C_{\text{end}\infty}. \tag{51}$$

In (44)–(51), the capacitances are given as follows: C_n by (25), C_3 by (15), $C_{3\infty}$ by (20), C_{end} by (35), and $C_{\text{end}\infty}$ by (39).

IDC with finger number $n = 2$:

1) Asymmetric strips, finite width terminals, Fig. 4(d):

$$C = C_{2a} + C_{\text{end}}. \tag{52}$$

2) Asymmetric strips, infinite width terminals, Fig. 4(c):

$$C = C_{2a} + C_{\text{end}\infty}. \tag{53}$$

3) Symmetric strips, finite width terminals:

$$C = C_{2s} + C_{\text{end}}. \tag{54}$$

4) Symmetric strips, infinite width terminals:

$$C = C_{2s} + C_{\text{end}\infty}. \tag{55}$$

In (52)–(55), the capacitances are given as follows: C_{2a} by (10), C_3 by (15), and as before, C_{end} by (35), and $C_{\text{end}\infty}$ by (39).

B. IDC on a Single-Layer Substrate

This IDC structure, Fig. 7(a), is the most studied one. In this case, the formulas for capacitance computation may be easily deduced from (44)–(55) in the $h_2 = h_3 = 0$ and/or $\epsilon_2 = \epsilon_1, \epsilon_3 = 1$ limits.

In Fig. 8, the dependence of the capacitance of the periodical section of IDC on stripwidth computed by (10) and by formulas given in [5] and [8] are depicted. The parameters used are as follows: $\epsilon_3 = 1, \epsilon_2 = \epsilon_1 = (28 \times 43)^{1/2}$ ($LiNbO_3$), $l = 1.5$ mm, $n = 12, 2g = 16$ μm, $t = 0.3$ μm, $h_1 = h_2 = 0.5$ mm. For these parameters and $2s = 2g = 16$ μm, the total capacitance, including external fingers and finger ends computed by (44), is 2.458 pF. The capacitance according to Alley's model [9] is 3.1 pF. The discrepancy is due to the ground plane assumed in Alley's model [9]. It is worthwhile to note that despite the differences in the mapping functions used by Wei [5] and (10), an excellent agreement is observed between the results of [5] and (10) for an infinitely thick substrate (without layers 2 and 3), Fig. 8. The larger capacitance computed based on the results of Wu *et al.* [8] is due to the model used in [8]. This problem will be discussed below.

A large number of experimental data are available in [19]. Table II displays a comparison of our results with the experimental and theoretical results of [19]. The modal parameters for comparison are as follows [19]: $l = 100$ μm, $2s = 2g = 10$ μm, $t = 5$ μm, $\epsilon_1 = 12.5$. The number of fingers are shown in the Table I.

Table II shows a comparison with the experimental and theoretical results presented in [20]. The modal parameters of IDC CAP1 and CAP2 are taken from [20]. For CAP1: $\epsilon_1 = 12.5, h_1 = 101$ μm, $l = 0.254$ mm, $2s = 20$ μm, $2g = 4.8$ μm, $t = 1.5$ μm, $n = 10$. For CAP2: $2g = 4.25$ μm, $2s = 12$ μm, $n = 19$, and the other parameters are as for CAP1.

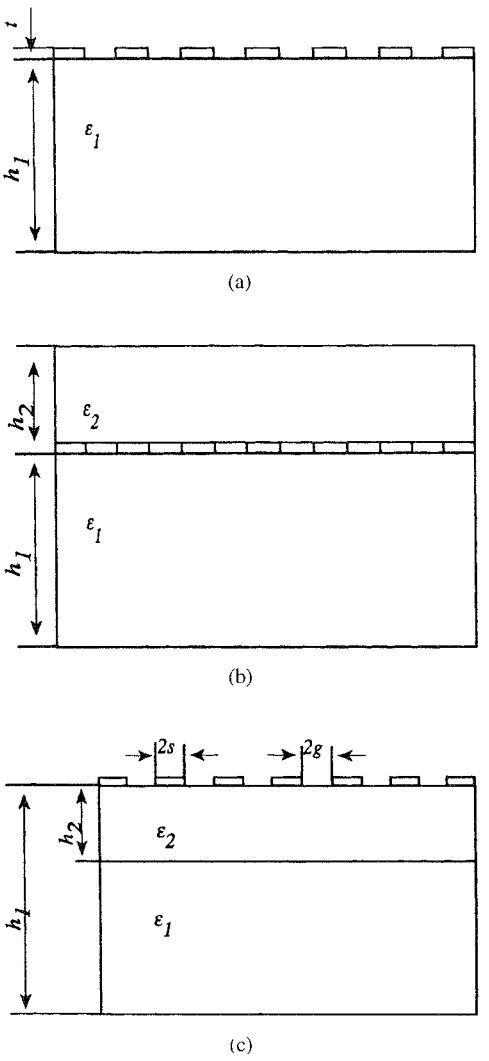

Fig. 7. Cross sections of single-layer substrate (a), dielectric covered (b), and superstrated (c) IDC.

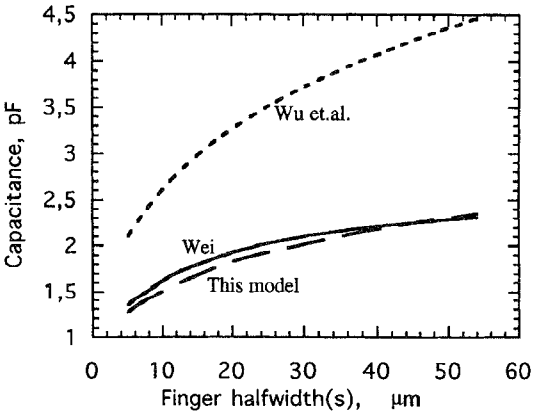

Fig. 8. Comparison with available models

C. IDC with a Dielectric Cover

There are not many reports in the literature concerning IDC with a dielectric layer on top of the metal strips. One recent publication [8] discusses ferroelectric films on top of superconducting strips. The modal parameters are as follows:

TABLE I
CAPACITANCE COMPARISON FOR DIFFERENT NUMBER OF FINGERS

n	5	10	20	50	205
C, pF, theory, [19]	0.036	0.079	0.165	0.425	2.215
C, pF, experiment, [19]	0.055	0.09	0.16	0.5	
C, pF, this method	0.0475	0.0945	0.183	0.453	1.86

TABLE II
COMPARISON OF THE CAPACITANCES OF IDC

C, pF, CAP1	C, pF, CAP2	Reference
0.247	0.607	Measured [20]
0.242	0.590	Computed [20]
0.283	0.587	This method

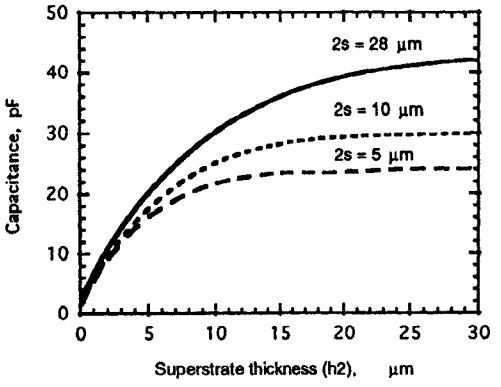

(a)

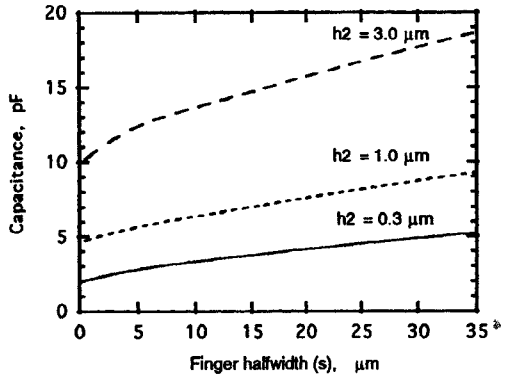

(b)

Fig. 9. Dependencies of the capacitance on thickness of covering dielectric (a), and halfwidth of the finger (b).

$\epsilon_1 = 24.5\ (LaAlO_3), h_1 = 0.5$ mm, $t = h_3 = 0.3\ \mu$m, $2s = 2g = 7.6\ \mu$m, $\epsilon_3 = 265$ (at temperature 78 K and zero bias), $n = 60, l = 0.501$ mm, $\epsilon_2 = 24.5$ and/or $h_3 = 0$. For this data the total capacitance computed using the present theory is 6.487 pF, including the "end" capacitance computed for $x = s/2 = 1.9\ \mu$m. According to [8], for the same data the computed capacitance without finger end contribution is 6.5 pF against 5.314 pF computed using the present theory. Hence, the capacitance without finger end contribution is elevated in [8]. This can easily be explained by referring to the field distributions in Fig. 2. In [8], a unit cell of IDC is distinguished as a three-strip coplanar waveguide. The capacitance is then presented as the half of the sum of $(n-1)$ coplanar waveguides. It can be seen from the comparison of the field distributions in IDC, Fig. 2(a), and in three-strip coplanar waveguide, Fig. 2(b), that there is additional fringing field at the external edges of the strips, Fig. 2(b), which for narrow strips will contribute into the capacitance substantially. There is no such a fringing field for the internal fingers of IDC and, in addition, the three-strip coplanar waveguide, Fig. 2(b), used in [8] as a "unit cell" for capacitance evaluation leads to repeated use of strip surface and hence elevated capacitances.

D. IDC with a Superstrate

It is worthwhile to study a ferroelectric film IDC with the structure shown in Fig. 7(c). The dielectric constant of the ferroelectric film is chosen to be $\epsilon_2 = 500$, and $\epsilon_1 = 24.5\ (LaAlO_3)$, i.e, $\epsilon_2 > \epsilon_1$. The other parameters are: $h_1 = 0.5$ mm, $t = 0.3\ \mu$m, $2g = 16\ \mu$m, $\epsilon_3 = 1, n = 12, l = 1.5$ mm, $x = s/2$, and $g_{\text{end}} = g$. The dependence of the total capacitance on the ferroelectric film thickness, h_2, is depicted in Fig. 9(a) with the stripwidth as a parameter, $2s = 2s_1 = 28$, 10, and 5 μm. For all thickness the capacitance tends to saturate when the film thickness approaches the gapwidth, $2g$, with the capacitance approaching the capacitance of the IDC on a homogeneous substrate with ϵ_2. The dependence of the capacitance on the stripwidth is shown in Fig. 9(b) with the ferroelectric film thickness as a parameter. The capacitance increases with s indicating a weak saturation where $s \equiv g$. This performance is explained as follows. An increase of stripwidth results in more field lines passing in the substrate, out of the high dielectric constant film.

VIII. CONCLUSION

Simple CAD-oriented analytical models have been developed for a large variety of IDC on three-layered substrates. It follows from the comparison of theory and experiment [1], [9], [19], [20], that these models can be used for frequencies up to the X-band. Poor accuracy is expected in the $2s/h < 1$ limit, where field lines become dominantly normal to the film/substrate interface and the magnetic wall approximation fails to work. In the case of computational problems, specially for ultra thin dielectric layers, $2s/h_i \gg 1$, approximations for the moduli of the elliptic integrals similar to (14) may be helpful. A simple series for computation of the ratio of the elliptic integral is given in [10]. Finally, models for the IDC on substrates with layer numbers $n > 3$ can easily be developed using the method presented in this paper.

ACKNOWLEDGMENT

The authors wishes to thank S. Rudner for helpful discussions.

REFERENCES

[1] B. C. Wadell, *Transmission Line Design Handbook*. Boston, MA: Artech House, 1991.
[2] R. K. Hoffman, *Handbook of Microwave Integrated Circuits*. Norwell, MA: Artech, 1987.
[3] E. Kollberg, "A dielectrically loaded slow-wave structure for travelling-wave maser applications," Chalmers University of Technology, Gothenburg, Sweden, Res. Rep. 72, 1966.
[4] T. Tammur, Ed., *Integrated Optics*. New York: Springer-Verlag, 1975.

[5] J. S. Wei, "Distributed capacitance of planar electrodes in optic and acoustic surface wave devices," *IEEE J. Quantum Electron.*, vol. QE-13, no. 4, pp. 152–158, 1977.
[6] O. G. Vendik, L. T. Ter-Martirosyan, A. I. Dedik, S. F. Karmenko, and R. A. Chakalov, "High-Tc superconductivity: New applications of ferroelectrics at microwave frequencies," vol. 144, pp. 33–43, 1993.
[7] R. M. Yandrofski, J. C. Price, F. Barnes, and A. M. Hermann, "Tunable microwave devices incorporating high temperature superconducting and ferroelectric films," Patent application, Int. Pub.. No. WO 94/13028, Int. Pub. date, 9 June, 1994.
[8] H.-D. Wu, Z. Zhang, F. Barnes, C. M. Jackson, A. Kain, and J. D. Cuchiaro, "Voltage tunable capacitors using high temperature superconductors and ferroelectrics," *IEEE Trans. Appl. Superconduct.*, vol. 4, no. 3, pp. 156–160, 1994.
[9] G. D. Alley, "Interdigital capacitors and their application to lumped element microwave integrated circuits," *IEEE Trans. Microwave Theory Tech.*, vol. MTT-18, no. 12, pp. 1028–1033, 1970.
[10] S. S. Gevorgian, P. Linnér, and E. Kollberg, "CAD models for shielded multilayered CPW," *IEEE Microwave Theory Tech.*, vol. 43, pp. 772–779, 1995.
[11] C. Veyers, and F. Hanna, "Extention of the application of conformal mapping techniques to coplanar lines with finite dimensions," *Int. J. Electronics*, vol. 48, no. 1, pp. 47–56, pp. 1980.
[12] G. Ghione and C. Naldi, "Coplanar waveguides for MMIC applications: Effects of upper shielding, conductor backing, finite extent ground planes, and line-to-line coupling," *IEEE Trans. Microwave Theory Tech.*, vol. MTT-35, no. 3, pp. 260–267, 1987.
[13] S. S. Gevorgian and I. G. Mironenko, "Asymmetric coplanar-strip transmission lines for MMIC and integrated optic applications," *Electron. Lett.*, vol. 26, no. 22, pp. 1916–1918, 1990.
[14] G. Ghione, and C.Naldi, "Analytical formulas for coplanar lines in hybrid and monolithic MICs," *Electron. Lett.*, vol. 20, no. 4, pp. 179–181, 1984.
[15] R. Schinzinger and P. A. Laura, *Conformal Mapping: Methods and Applications*. The Netherlands: Elsevier, 1991.
[16] L. J. P. Linnér, "A method of computation of the characteristic immittance matrix of multiconductor striplines with arbitrary widths," *IEEE Trans. Microwave Theory Tech.*, vol. MTT-22, pp. 930–937, 1974.
[17] H. Kober, *Dictionary of Conformal Representations*. New York: Dover, 1957.
[18] A. P. Prudnikov, Yu. A Brychkov, and O. I. Marichev, *Integrals and Series*, vol. 1. NY: Gordon and Breach, 1986.
[19] E. Pettenpaul, H. Kapusta, A. Weisgerber, H. Mampe, J. Luginsland, and I. Wolff, "CAD models of lumped elements on GaAs up to 18 GHz," *IEEE Trans. Microwave Theory Tech.*, vol. 36, no. 2, pp. 294–304, 1988.
[20] R. Esfandiari, D. W. Maki, and M. Siracusa, "Design of interdigitate capacitors and their application to gallium arsenide monolithic filters," *IEEE Trans. Microwave Theory Tech.*, vol. 31, no. 1, pp. 57–64, 1983.
[21] M.-H Mao, R.-B. Wu, C.-H Chen, and C.-H. Lin, "Characterization of coplanar waveguide open end capacitance—Theory and experiment," *IEEE Trans. Microwave Theory Tech.*, vol. 42, no. 6, pp. 1016–1024, 1994.
[22] S. Gevorgian, A. Deleniv, T. Martinsson, E. Kollberg, and I. Vendik, "Modeling open ends in coplanar waveguides," to be published.

Spartak S. Gevorgian (M'96) received the electronics engineering degree from the Engineering University of Armenia, Yerevan, in 1972, and the Doctor of Sciences and Ph.D. degrees from Leningrad Electrical Engineering University, St. Petersburg, Russia, in 1977 and 1991, respectively.

From 1977 to 1988, he was with the Engineering University of Armenia as a reader (docent), and since 1991 has been a Professor in the Electrical Engineering University of St. Petersburg, Russia. From 1981 to 1982, he had a scholarship in the University College, London. His fields of interests are in microwave integrated circuits, integrated optics, and optically controlled microwave devices. Since 1993, he is with the Department of Microwave Technology, Chalmers University of Technology, Sweden. Presently, he is engaged in the development of HTSC and integrated HTSC/ferroelectric microwave devices. He is author of a monograph ("Glass based integrated optical devices," St. Petersburg, Russia), and more than 100 scientific papers.

Torsten Martinsson was born in Sweden, in 1969. He received the M Sc. degree in engineering physics from Chalmers University of Technology, Gothenburg, Sweden, in 1995, where he is working toward the Ph.D. degree in microwave technology.

He is currently working with modeling and experimental study of HTSC microwave circuits. His emphasis is on coplanar waveguides and resonators, discontinuities in CPW, and interdigital capacitors.

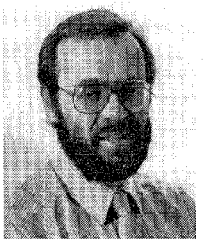

Peter L. J. Linnér (S'68–M'74–SM'87) was born in Växjö, Sweden, on April 4, 1945. He received the M.Sc. and Ph.D. degrees in electrical engineering from Chalmers University of Technology, Gothenburg, Sweden, in 1969 and 1974, respectively.

In 1969, he became a Teaching Assistant in mathematics and telecommunications at Chalmers University of Technology. In 1973, he joined the research and teaching staff of the Division of Network Theory at the same university with research interests in the areas of network theory, microwave engineering, and computer-aided design methods. In 1974, he moved to the MI-division, Ericsson Telephone Company, Mölndal, Sweden, where he was a systems engineer and project leader in several military radar projects. He returned to Chalmers University of Technology as a Researcher in the areas of microwave array antenna systems. Since 1981, he has been a University Lecturer in telecommunications. For part of 1992, he spent a period at the University of Bochum, Bochum, Germany, as a Guest Researcher. His current interest is in the application of computer-aided network methods in the area of microwave and antenna technology with current emphasis on superconduction.

Erik Ludvig Kollberg (M'83–SM'83–F'91) received the Teknologie Doktor degree from Chalmers University of Technology, Göteborg, Sweden, in 1970.

He became a Professor at the School of Electrical and Computer Engineering in 1980, and was the acting Dean of Electrical and Computer Engineering from 1987 to 1990. From 1967 to 1987, one of his major responsibilities was the development of radio astronomy receivers working from a few GHz up to 250 GHz for the Onsala Space Observatory telescopes in Sweden and in Chile. From 1963 to 1976, he conducted research on low-noise maser amplifiers. Various types of masers were developed for the frequency range 1 GHz to 35 GHz. Eight such masers are, or have been, used for radio astronomy observations at the Onsala Space Observatory. In 1972, he began research on low-noise millimeter wave Schottky diode mixers, and 1982 also on superconducting quasiparticle mixers. This research covered device properties as well as mixer development for frequencies from about 30 GHz to 750 GHz. In 1980, he began research on GaAs millimeter wave Schottky diodes, and since 1986, he has been engaged in research on quantum well devices and three terminal devices such as FET's and HBT's. Present HFET-devices can operate up to approximately 350 GHz. Recently, he has made contributions to the limitation in performance of **varactor** multipliers and hot electron mixers. He was a Guest Professor to Ecole Normal Superieure, Paris, France, in the summer's of 1983, 1984, and 1987, and acted as the Dean of the School of Electrical and Computer Engineering from 1987 to 1990. From September 1990 to March 1991, he was invited as a Distinguished Fairchild Scholar at the California Institute of Technology. He has published 160 scientific papers.

Dr. Kollberg received the 1982 Microwave Prize given at the 12th European Microwave Conference in Helsinki, Finland, and the Gustaf Dahlén gold medal 1986.